Radioprotective effects of centipedegrass extract on NIH-3T3 fibroblasts via anti-oxidative activity

SEONG HEE KANG[1,2*], DONG-HO BAK[1*], SEUNG SIK LEE[1,3], HYOUNG-WOO BAI[1,3], BYUNG YEOUP CHUNG[1] and BO SUN KANG[2]

[1]Research Division for Biotechnology, Advanced Radiation Technology Institute (ARTI), Korea Atomic Energy Research Institute (KAERI), Jeongeup, Jeollabuk 56212; [2]Department of Radiological Science, Konyang University, Daejeon 35365; [3]Radiation Biotechnology and Applied Radioisotope Science, University of Science and Technology (UST), Daejeon 34113, Republic of Korea

Abstract. Centipedegrass originates from China and South America, and has been reported to contain several C-glycosyl flavones and phenolic compounds, including maysin and luteolin. The present study aimed to investigate the radioprotective activity of centipedegrass extract (CGE) in radiation exposed-fibroblasts and to assess the affected molecular pathway. The radioprotective effects of CGE were determined in NIH-3T3 cells using Cell Counting Kit-8 and morphological changes were observed. Reactive oxygen species (ROS) levels and the apoptotic profile of NIH-3T3 cells were also measured. The expression levels of B-cell lymphoma-2 (Bcl-2) family proteins [Bcl-2, Bcl-2 like protein 4 (Bax), Bcl-2-associated death promoter (Bad), caspase-3, poly(ADP-ribose) polymerase (PARP)], AKT and MAPK family proteins (ERK, p38 and JNK) were measured *in vitro*. The results demonstrated that when 3T3 fibroblasts pretreated with CGE were subjected to H_2O_2-induced cell damage, their viability was significantly decreased. Additionally, CGE pretreatment decreased ROS levels and the protein expression levels of cleaved PARP upon H_2O_2 treatment, indicating that CGE induced cytoprotective effects against H_2O_2-induced oxidative stress. Moreover, significant protective effects of CGE against intracellular ROS, induced upon exposure to ionizing radiation (IR), were observed. The protective effects of CGE pretreatment were also determined by morphological observation of NIH-3T3 cells following exposure to IR. CGE pretreatment increased the expression levels of anti-apoptotic signals (Bcl-2, p-BAD) and decreased the levels of pro-apoptotic signals (Bax, Bad), and led to cleavage of PARP and caspase-3 proteins. Additionally, in cells pretreated with CGE, the phosphorylation of AKT and ERK was increased and that of p38 and JNK was decreased compared with in cells subjected only to IR. These results indicated that CGE may act as a radioprotector due to its anti-oxidative activity, restoring cell homeostasis and redox balance in radiation-exposed fibroblast cells. Therefore, it could be suggested that CGE may be an effective candidate in the treatment of oxidative stress-related diseases and in radioprotection.

Correspondence to: Dr Bo Sun Kang, Department of Radiological Science, Konyang University, 158 Gwanjeodong-ro, Daejeon 35365, Republic of Korea
E-mail: bskang@konyang.ac.kr

Dr Byung Yeoup Chung, Research Division for Biotechnology, Advanced Radiation Technology Institute (ARTI), Korea Atomic Energy Research Institute (KAERI), 29 Geumgu-gil, Jeongeup, Jeollabuk 56212, Republic of Korea
E-mail: bychung@kaeri.re.kr

*Contributed equally

Abbreviations: Bcl-2, B-cell lymphoma-2; Bax, Bcl-2 like protein 4; Bad, Bcl-2-associated death promoter; CGE, centipedegrass extract; H2DCFDA, 2,7-dichlorodihydrofluorescein-diacetate; DHE, dihydroethidium; DMSO, dimethyl sulfoxide; DMEM, Dulbecco's modified Eagle's medium; EA, ethyl acetate; FBS, fetal bovine serum; HRP, horseradish peroxidase; IR, ionizing radiation; ROS, reactive oxygen species; MeOH, methanol; PARP, poly(ADP-ribose) polymerase; RISR, radiation-induced skin reaction; RT, radiation therapy

Introduction

Centipedegrass belongs to the genus *Eremochloa* (Poaceae), which includes eight species that inhabit China and Southeast Asia, and is one of the most popular grasses in South America (1). It contains C-glycosyl flavones and phenolic constituents as its common structural skeleton, which is biologically active (2). In a previous study, we isolated and analyzed the extract from centipedegrass, and found that these components included maysin, and maysin derivatives such as luteoin-6-C-boivinopyranose, luteolin, Isoorientin, rhamnosylisoorientin, and derhamnosylmaysin (3). Particularly, centipedegrass extract (CGE), a flavonoid-rich chemical compound extracted from centipedegrass, has been reported to demonstrate free radical-scavenging activity *in vitro* biochemical assays using DPPH-radical scavenging activity (4). It was

also reported that maysin (a C-glycoside flavone from centipe-degrass) and its precursor chemical components could exhibit anti-oxidative activity via DPPH radical scavenging *in vitro* antioxidant model (5), and protect SK-N-MC cell lines against inhibition of H_2O_2-induced apoptotic cell death (6). Despite these health benefits of maysin and flavonoid derivatives, its cytoprotective effects against ionizing radiation (IR)-induced cell death in fibroblasts and the underlying mechanisms have not been elucidated yet.

Cancer remains a big challenge in global healthcare because it is one of the most rampant causes of death. Radiation therapy (RT) is one of the most important treatment strategies used in the treatment of more than two thirds of cancer cases worldwide (7). Advances in technology over the last decades have prompted the development of 3-dimensional conformal RT techniques, including intensity-modulated radiation therapy and stereotactic body radiation therapy (8). In addition to these advanced medical technologies, therapeutic strategies in radiation oncology have grown significantly with advances in physiology, immunology, and molecular biology, allowing us to explore the treatment outcome from a better, all-inclusive perspective, and perform radiotherapy more efficiently.

However, long-term stimulation of IR in human tissues unavoidably leads to the development of free radical pathology. Generally, IR affects the body of patients indirectly; for example, upon interaction with water molecules in cells exposed to radiation, large amounts of free radicals and reactive oxygen species (ROS) are produced, which oxidize cellular components, causing cellular damage (9). The cells that are exposed to radiation respond via generation of antioxidant enzymes depending on the degree of exposure, followed which free radical-induced damage to the cellular structure is minimized or eliminated (10). However, when ROS are produced due to exposure of the body to radiation and excessive amounts of free radicals, they cannot be completely removed by intrinsic antioxidative enzymes.

Radiation-induced skin reaction (RISR) is one of the main side effects of radiotherapy, and more than 95% of patients undergoing RT experience tissue damage (11). Moreover, acute RISR often has a big impact on the progress of RT due to limitation of the total therapeutic dose or breaks in radiotherapy (12). Radiation-induced oxidative stress is known to be the main cause of RISR (13). Oxidative stress induced by IR results in damages of DNA, lipids, and proteins. The harmful effects stimulate early transcription factors and molecular signals leading to cellular damage. As a result, it causes damage to the skin tissue (14). Thus, in radiotherapy, IR-induced oxidative stress is an important variable before and after IR, and it is essential to scavenge the IR-induced free radicals or ROS to reduce/mitigate the damage caused by radiation.

Fibroblasts, the main type of cells constituting the dermal skin, play important roles in the development of healthy skin by producing the extracellular matrix and collagen. The occurrence of damaged fibroblasts, resulting in the presence of low levels of extracellular matrix proteins, is the result of skin aging, and is consequently responsible for the formation of wrinkles (15). IR-induced oxidative stress has been reported to cause damage with ROS inducing apoptosis in a variety of cells, including fibroblasts and keratinocytes, thereby reducing cell numbers and regenerative capacity (16).

Additionally, persistent oxidative stress during RT can lead to severe cellular damage and irreversible tissue conditions, which makes tissue regeneration impossible (17). This consideration marked the beginning of the active development of a radioprotector for the prevention and treatment of IR-induced free radical pathology with the use of antioxidant agents (18). Studies involving the use of vitamins, amino acids, animal- and plant-based agents containing antioxidant enzymes are considered to be highly significant but less developed in the field of radiobiology. Considering the lack of efficient radioprotective agents made of natural raw materials, many studies have been undertaken with the purpose of finding radioprotective agents (19,20).

In this study, CGE, which contains flavonoid derivatives, was evaluated for its radioprotective effects against IR-induced cell damage in NIH-3T3 fibroblast cells.

Materials and methods

Preparation of CGE. CGE was prepared using the method described in our previous report (21). Briefly, seeds of centipe-degrass imported from the Fukukaen Nursery (Blu Co. Ltd.) were cultivated at the Korea Atomic Energy Research Institute in 2016 (KAERI). The leaves of the centipedegrass were harvested and stored at -80˚C until use. Dry leaves of centipede (5 kg) were crushed in a Wiley mill (Indian Weiber) and filtered through a sieve of pore size 420 μm. The final sample of ground leaves (1 kg) was extracted thrice using 80% methanol (MeOH, 100 liters; Merck) for 24 h with constant shaking at ambient temperature in the dark. The extracts were filtered using a No. 2 filter paper (Advantech) and concentrated in vacuum. MeOH extracts were fractionated successively using n-hexane and ethyl acetate (EA). The layer separated using EA was concentrated in vacuum and the dried compound was dissolved in MeOH. The active MeOH extracts were diluted with 20% MeOH and chromatographed on a Toyopearl HW-40C resin (Tosoh Corp.) column using 70% MeOH (elution volume, 700 ml). Fractions were evaporated and lyophilized. The dried extract was diluted in dimethyl sulfoxide (DMSO) to carry out further experiments. Lastly, to confirm the active substances content, maysin, and maysin derivatives (the active ingredient of CGE) were confirmed by high-performance liquid chromatography/mass (HPLC-MS) analysis as previously described method (3).

Chemicals and reagents. All the chemicals and reagents were used without further purification. A cell counting kit-8 was purchased from Sigma-Aldrich; Merck KGaA. Anti-AKT (#4691), anti-p-AKT (#4060), anti-ERK (#4695), anti-p-ERK (#4377), anti-p38 (#9212), anti-p-p38 (#9215), anti-JNK (#9252), anti-p-JNK (#9251), anti-caspase-3 (#9662), anti-cleaved caspase-3 (#9664), anti-Bcl-2 (#2870), anti-Bax (#5023), anti-Bad (#9292), anti-p-Bad (#9291), anti-poly(ADP-ribose) polymerase (PARP) (#9532), anti-cleaved PARP (#9541), anti-GAPDH (#2118), and anti-α-tubulin (#2144) were purchased from Cell Signaling Technology, Inc. Dulbecco's modified Eagle's medium (DMEM), penicillin/streptomycin (P/S), and fetal bovine serum (FBS) were purchased from Lonza. Annexin V and oxidative stress kits were purchased from Millipore.

Cell culture. The NIH-3T3 cell line (mouse, fibroblast) was obtained from the Korean Cell Line Bank (Seoul, Korea). The cells were cultured under sterile conditions at 37°C in a humid environment containing 5% CO_2. The culture medium consisted of DMEM supplemented with FBS (10%), glutamine (4 mM), and penicillin/streptomycin (1%).

Morphological analysis and cell viability. The morphology of NIH-3T3 cells was monitored using an Olympus IX71 fluorescence microscope (Olympus Corp.). In order to determine the half-maximal inhibitory concentration (IC_{50} value) of H_2O_2 or the effects of CGE on NIH-3T3 cells, $1x10^4$ cells (from a single-cell suspension) were seeded into individual wells of 96-well plates and incubated for 24 h at 37°C before H_2O_2 treatment (125-500 μM). For H_2O_2 treatment, each well received a 1:2 sequential dilution of H_2O_2 from 500 μM to 125 μM. Alternatively, CGE was also added sequentially to the wells (25-100 μg/ml), after which, the cells were incubated for 24 h. 0.1% DMSO was used as vehicle control. CCK-8 solution was added to each well and the plates were incubated for 1 h at 37°C to allow the reaction to take place before removal of the culture medium. Cell viability was determined using a spectrophotometer and the absorbance was measured at 450 nm (Tecan). The cell viability for each group was calculated as a percentage of that of the control group.

Measurement of intracellular ROS levels. NIH-3T3 cells ($1x10^5$ cells/well for fluorescence and oxidative stress assays, $1x10^4$ cells for the DCF-DA assay) grown on coverslips in 6-well/96-well plates were incubated with CGE (100 μg/ml) for 24 h at 37°C before H_2O_2 treatment (500 μM) or IR exposure (4 Gy). The following procedures were conducted: i) DCF-DA staining: the cells were treated with DCF-DA according to the manufacturer's instructions and examined using a fluorescence microscope or microplate reader (excitation: 485 nm, emission: 535 nm). ii) Oxidative stress assay: Cellular populations undergoing oxidative stress were measured quantitatively using the Muse™ Cell Analyzer and Muse™ Oxidative Stress kit (EMD Millipore). According to the manufacturer's protocol, the cells were detached, resuspended to obtain $1x10^6$ cells/ml and incubated at 37°C for 30 min with the Muse™ Oxidative Stress working solution. The number of oxidized cells was counted using the Muse™ Cell Analyzer based on the intensity of red fluorescence. The results were obtained from four independent experiments.

Apoptotic assay. NIH-3T3 cells ($3x10^5$ cells/well) grown in a 65-mm culture dish were incubated with CGE (100 μg/ml) for 24 h at 37°C before H_2O_2 treatment (500 μM). The following procedures were conducted to determine apoptosis in the cells: i) Fluorescence imaging: Cells were incubated with DAPI according to the manufacturer's instructions and examined using a confocal microscope (Zeiss AG). ii) Annexin V assay: To quantitatively analyze the apoptotic and necrotic dead cells, Muse Annexin V and Dead Cell Assay kits (MCH100105; EMD Millipore) were used. The cells were harvested and washed with DPBS. The cells were then stained with Annexin V and the Dead Cell reagent for 20 min, following which flow cytometric assessment was performed using the Muse™ Cell Analyzer. The number of apoptotic cells were expressed as the percentage of the live, early/late apoptotic, and dead cells, which was determined by the Muse analysis software (Muse 1.1.2; EMD Millipore).

gamma-ray irradiation. gamma-ray irradiation was performed at room temperature at the dose rate of 1 Gy/min using a Cs^{137} gamma cell (MDS Nordion). The cells were directly irradiated in the flasks. After irradiation, they were incubated at 37°C and 5% CO_2 until they could be harvested for direct experimentation or were stored at appropriate temperatures until further use.

Clonogenic assay. The NIH-3T3 cells (1,000 cells/well) grown on coverslips in 6-well plates were incubated with CGE (100 μg/ml) for 24 h at 37°C prior to IR exposure (4 Gy). After exposure to various doses (1-12 Gy) of gamma-rays, the cells were incubated with fresh media for 7 days, fixed using pure MeOH for 20 min at room temperature and stained using Wright stain (Thermos Fisher Scientific, Inc.) for 20 min. The number of colonies containing more than 50 cells was counted.

Western blot analysis. NIH-3T3 cells were washed with PBS and lysed with radioimmunoprecipitation assay buffer. The proteins (30-50 μg) were separated via 10% sodium dodecyl sulfate-polyacrylamide gel electrophoresis and were then transferred onto polyvinylidene difluoride membranes. The membranes were blocked with 5% non-fat dry milk for 1 h at room temperature and then incubated overnight with 1:1,000-diluted primary antibodies at 4°C. The membranes were washed with tris-buffered saline and incubated with horseradish peroxidase (HRP)-conjugated secondary antibodies (anti-rabbit IgG, HRP-linked antibody, #7074; Cell Signaling Technology, Inc.) for 2 h at room temperature. The proteins were then visualized using an enhanced chemiluminescence reagent (Millipore Corp.) and exposure to an X-ray film.

Statistical analysis. Each experiment was performed at least three times, and the results were expressed as the mean ± standard deviation. For multiple comparisons, one-way analysis of variance was used followed by Tukey's multiple comparisons test. $P \leq 0.05$ was considered to indicate a statistically significant difference.

Results

CGE protects NIH-3T3 cells from H_2O_2-induced damage. The cytotoxic effect of CGE was determined by measuring the viability of cells treated with increasing concentrations of CGE using a colorimetric CCK-8 assay. Stimulation with CGE did not have a significant effect on cell viability at any tested concentration (25-100 μg/ml) over a period of 24 h (Fig. 1A). Thus, all the subsequent experiments were conducted at the concentration of 100 μg/ml. Next, the effect of H_2O_2 (potent pro-oxidant)-induced damage in NIH-3T3 cells was examined to determine the protective effect of CGE against oxidative stress. It was observed that the viability of H_2O_2-stimulated NIH-3T3 cells had reduced to 65 and 43% at the concentrations of 250 and 500 μM, respectively (Fig. 1B). Therefore, the cell viability was evaluated next, and the cellular morphologies
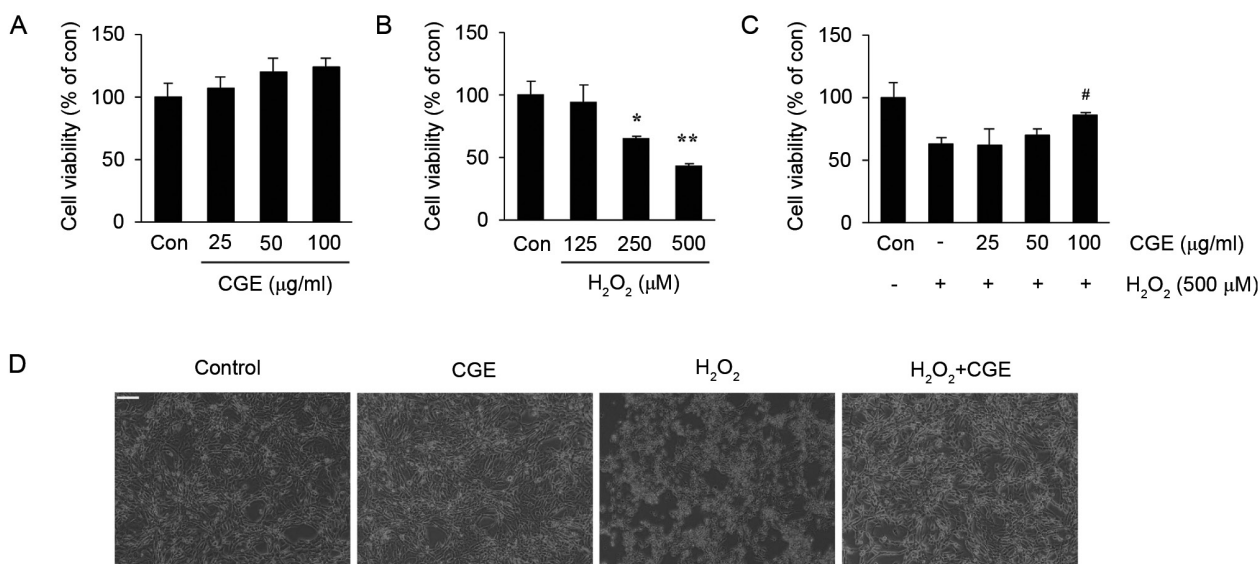
Figure 1. CGE protects NIH-3T3 fibroblast cells from H_2O_2-induced damage. (A) NIH-3T3 cells treated with increasing concentrations of CGE or a vehicle control for 24 h. (B) NIH-3T3 cells stimulated with H_2O_2 (125-500 μM) for 24 h. Cell viability was assessed by the CCK-8 assay. (C and D) NIH-3T3 cells were treated with CGE (100 μg/ml) for 24 h before H_2O_2 stimulation (500 μM). After 24 h, the effects of CGE on (C) cell viability and (D) protection of the NIH-3T3 cells were assessed with an inverted phase-contrast microscope. Scale bar, 200 μM. Data are presented as mean $\pm$ SD. *P$\leq$0.05, **P$\leq$0.01 vs. Co; $^{\#}$P$\leq$0.05 vs. H_2O_2 only. CGE, centipedegrass extract; H_2O_2, hydrogen peroxide; Con, control; SD, standard deviation.

were observed to examine whether CGE exhibits any protective effect in NIH-3T3 cells stimulated with 500 μM of H_2O_2. As shown in Fig. 1C, CGE exhibited a protective effect on H_2O_2-induced cytotoxicity; additionally, this effect was confirmed by a decrease in the irregular morphology observed due to H_2O_2-induced cellular damage (Fig. 1D). These data indicate that CGE could inhibit H_2O_2-induced cytotoxicity in NIH-3T3 cells.

CGE regulates H_2O_2-mediated intracellular ROS levels. To investigate the effect of CGE on ROS levels, we determined whether CGE treatment could attenuate H_2O_2-mediated oxidative stress. The NIH-3T3 cells were stimulated with H_2O_2 in the presence or absence of CGE, after which, the production of ROS was observed using the fluorescent probe 2,7-dichloro-dihydrofluorescein-diacetate (H2DCFDA) of the cellular ROS detection kit. Treatment with H_2O_2 alone resulted in robust intracellular generation of ROS, whereas H_2O_2-induced ROS generation in NIH-3T3 cells was significantly attenuated by CGE treatment (Fig. 2A). Moreover, decrease in the oxidative stress was quantified via the dihydroethidium (DHE) reaction. DHE is cell permeable and is considered to react with superoxide anions, thus undergoing oxidation upon binding to DNA (22). As shown in Fig. 2B, CGE treatment led to a decrease in the number of cells demonstrating high ROS production. A significant decrease in the oxidative stress was observed in the NIH-3T3 cells. These results implied that pretreatment with CGE reduces the accumulation of intracellular ROS in NIH-3T3 cells.

CGE inhibits H_2O_2-induced cell death in NIH-3T3 cells. To elucidate the protective effects of CGE against H_2O_2-induced damage in NIH-3T3 cells, the effects of CGE on H_2O_2-mediated apoptosis were investigated. The results of the cell nucleus staining showed that treatment with H_2O_2

alone had significantly increased the number of cells with condensed or blebbing nuclei. Contrarily, when cells were pretreated with CGE, the nuclear damages were markedly reduced (Fig. 3A). The results of the flow cytometry consistently indicated that H_2O_2 treatment had increased the population of Annexin V$^+$/PI-apoptotic cells. However, as shown in Fig. 3B, pretreatment of the cells with CGE prior to their exposure to H_2O_2 led to effective protection of the cells against apoptosis. Likewise, results of western blotting indicated a significant increase in the expression of cleaved PARP, a well-known substrate of caspase-3 in the apoptotic cell death, compared to that of the control. However, in alignment with previous results, Fig. 3C showed that the H_2O_2-induced PARP degradation was reduced by pretreatment of the cells with CGE. Taken together, these results indicated that CGE pretreatment could inhibit H_2O_2-induced apoptotic cell death in NIH-3T3 cells.

CGE increases the viability of IR-exposed NIH-3T3 cells. To investigate whether the IR-induced cell damage could be prevented by CGE pretreatment, first, the morphological changes in NIH-3T3 cells were evaluated. As shown in Fig. 4A, it was confirmed that pretreatment with CGE could decrease the irregular morphology observed in IR-exposed NIH-3T3 cells. In addition, to further investigate the relationship between cell fractions retaining reproductive integrity and absorbed radiation dose, the clonogenic survival curves were determined. The cell survival fraction in the IR-exposed NIH3/T3 cells was evaluated by the cell survival curve. As shown in Fig. 4B, IR caused cell death in proportion to the amount of exposure. However, pretreatment with CGE significantly increased cell viability 24 h after irradiation over the full range of doses. Particularly, the 50% lethal dose (LD 50%) of cells pretreated with CGE reduced from 4.51 to 3.41 Gy. Previous experiments have confirmed that CGE is capable of inhibiting H_2O_2-induced cell damage. As IR has been shown
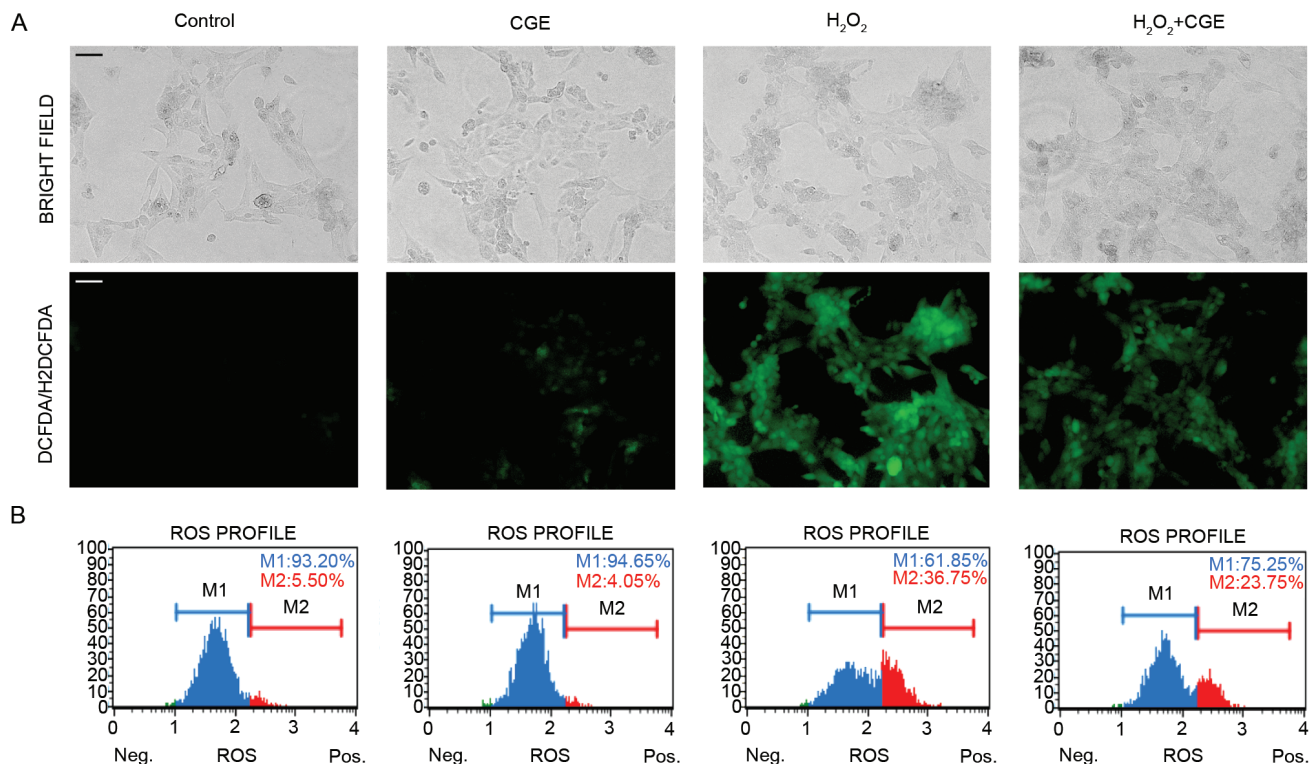
Figure 2. CGE regulates H_2O_2-mediated intracellular ROS generation. NIH-3T3 cells were treated with CGE (100 μg/ml) for 24 h and stimulated with H_2O_2 (500 μM) for 4 h. (A) Cells were stained with H2DCFDA for 30 min to measure intracellular hydrogen peroxide (H_2O_2) levels using fluorescence microscopy. Scale bar, 25 μM. (B) Cells were treated with DHE for 30 min to measure intracellular superoxide (O_2^-) levels and were analyzed using a Muse™ Cell analyzer. Representative oxidative stress plots for the NIH-3T3 cells. CGE, centipedegrass extract; H_2O_2, hydrogen peroxide; ROS, reactive oxygen species; H2DCFDA, 2,7-dichlorodihydrofluorescein-diacetate; DHE, dihydroethidium; Con, vehicle control (0.1% DMSO).

to adversely affect cells via ROS generation, we investigated whether one possible mechanism for the cytoprotective effect of CGE against damages induced by IR is based on its ROS scavenging capacity. To investigate whether CGE could reduce IR-induced ROS generation, H2DCFDA was used for a fluorescence assay. Fig. 4C represents the quantitative analysis of the cellular ROS levels. When the cells were pretreated with CGE, the fluorescence intensity of H2DCFDA was found to be significantly reduced. These results demonstrated that IR caused cell damage by inducing overproduction and accumulation of intracellular ROS, which was effectively prevented by CGE.

CGE inhibits apoptosis in IR-exposed NIH-3T3 cells via regulation of the ERK-, p38-, JNK-MAPKs signaling. Radiation is known to mainly induce intrinsic apoptotic cascades such as the mitochondrial release of cytochrome c and subsequent formation of the apoptosome. However, depending on dosage and cell type, the extrinsic apoptotic pathway might also induce cell death (23). In this study, to explore the possible molecular mechanism underlying the radioprotective effects of CGE in NIH-3T3 cells exposed to radiation, first, the protein expression related to the intrinsic apoptotic pathway was examined. The intrinsic apoptotic pathway is controlled and regulated by the activities of the members of the Bcl-2 protein family involved in mitochondrial membrane permeability and which may be pro-apoptotic or anti-apoptotic (24). As shown in Fig. 5, radiation activates the expression of the pro-apoptotic Bcl-2 proteins Bax (Bcl-2 like protein 4), Bad,

PARP, and cleaved caspase-3, whereas it inhibits the expression of the anti-apoptotic protein Bcl-2. However, when cells were pretreated with CGE, the expression of anti-apoptotic proteins was significantly decreased. Additionally, pretreatment with CGE has been shown to lead to phosphorylation of BAD by inducting AKT phosphorylation, thereby rendering these signal proteins inactive in apoptotic processes.

Previous studies have reported that exposing cells to IR and various other toxic stresses can induce simultaneous target activation of multiple MAPK pathways (25). This has been related with the factor-mediated regulation of various cell longevity factors such as proliferation, differentiation, aging, and apoptosis. Thus, the expression of MAPK family (ERK1/2, p38 and JNK), which plays a role in the extrinsic apoptotic pathway, in IR-exposed cells was explored using immunoblot analysis. Fig. 6A and B shows that the expression levels of p-ERK in IR-exposed NIH-3T3 cells were downregulated whereas those of p-JNK and p-p38 were upregulated. Conversely, these changes in the expression levels were largely alleviated by pretreatment with CGE. Collectively, these results supported the hypothesis that pretreatment with CGE protects the NIH-3T3 cells against IR-induced cell death via inhibition of the intrinsic apoptotic pathway as well as the regulation of the ERK-, p38-, JNK-MAPKs signaling.

Discussion

ROS plays diverse roles depending on the concentration present in cells. ROS participate in the molecular signaling
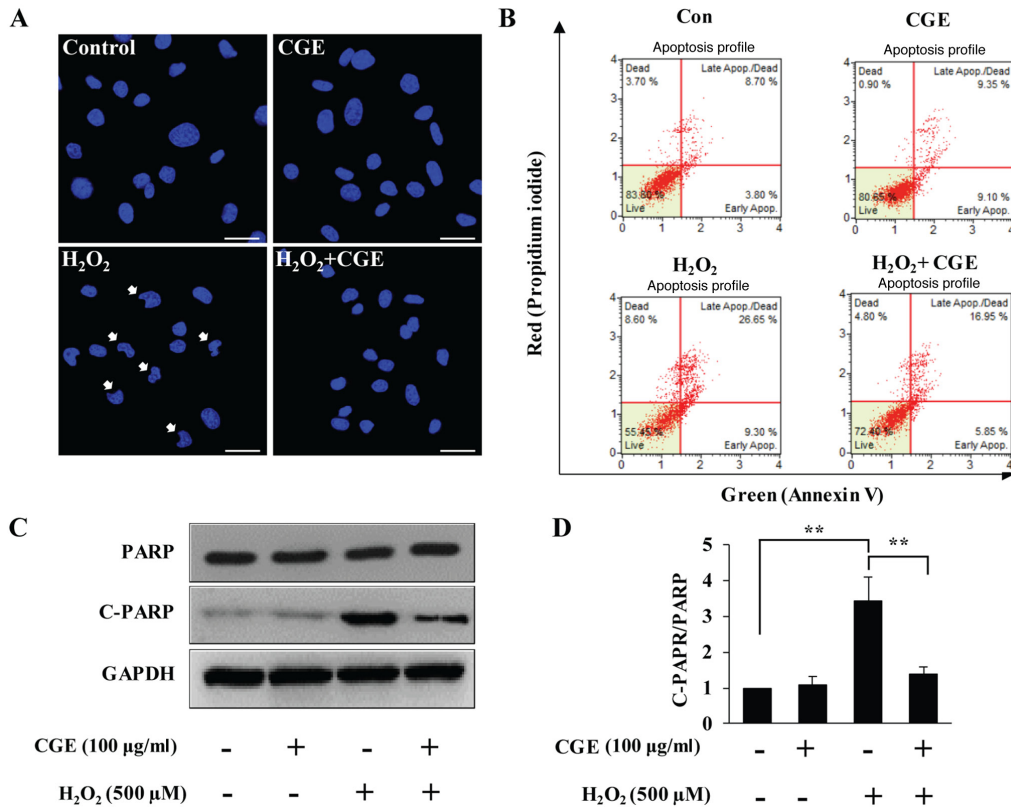
Figure 3. CGE suppresses H$_2$O$_2$-induced apoptosis. NIH-3T3 cells were treated with or without CGE for 24 h and incubated with H$_2$O$_2$ (500 μM) for 24 h. (A) Changes in nuclear morphology examined by Hoechst 33342 nuclear staining. Arrows indicate apoptotic nuclei. Scale bar: 50 μm. (B) Cells stained with Annexin V-FITC and analyzed using a cell sorting system with Muse™. (C) Whole cell lysates prepared and immunoblotted with antibodies against cleaved PARP. (D) Western blots were analyzed quantitatively. The band intensities were normalized to GAPDH. Data are presented as mean ± SD. **P≤0.01 vs. H$_2$O$_2$ only. CGE, centipedegrass extract; H$_2$O$_2$, hydrogen peroxide; ROS, reactive oxygen species; PARP, poly(ADP-ribose) polymerase; GAPDH, glyceraldehyde 3-phosphate dehydrogenase; Con, vehicle control (0.1% DMSO); SD, standard deviation.
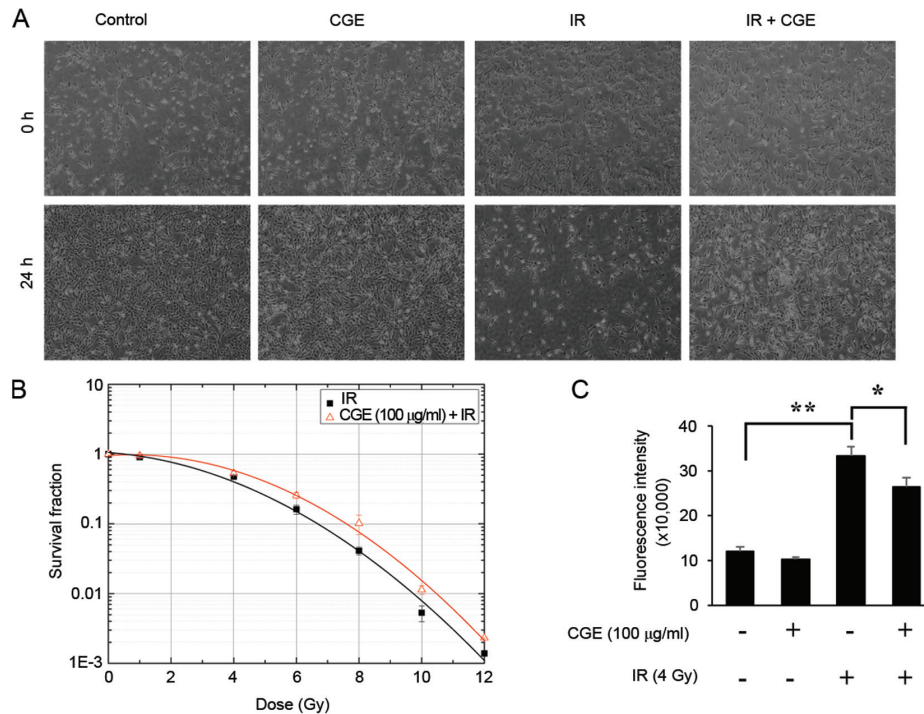

Figure 4. CGE increases the viability of IR-exposed NIH-3T3 cells. (A) The protection of NIH-3T3 cells after their exposure to IR was assessed using an inverted phase-contrast microscope. Magnification, x100. (B) Clonogenic assay was performed to evaluate NIH-3T3 cell viability. (C) NIH-3T3 cells were stained with H2DCFDA for 30 min to measure intracellular H$_2$O$_2$ levels using a microplate reader. The bar graph presents a quantitative analysis of the generation of intracellular hydrogen peroxide. Data are presented as mean ± SD. *P≤0.05, **P≤0.01 vs. IR only. CGE, centipedegrass extract; H$_2$O$_2$, hydrogen peroxide; IR, ionizing radiation; H2DCFDA, 2,7-dichlorodihydrofluorescein-diacetate; Con, vehicle control (0.1% DMSO); SD, standard deviation.
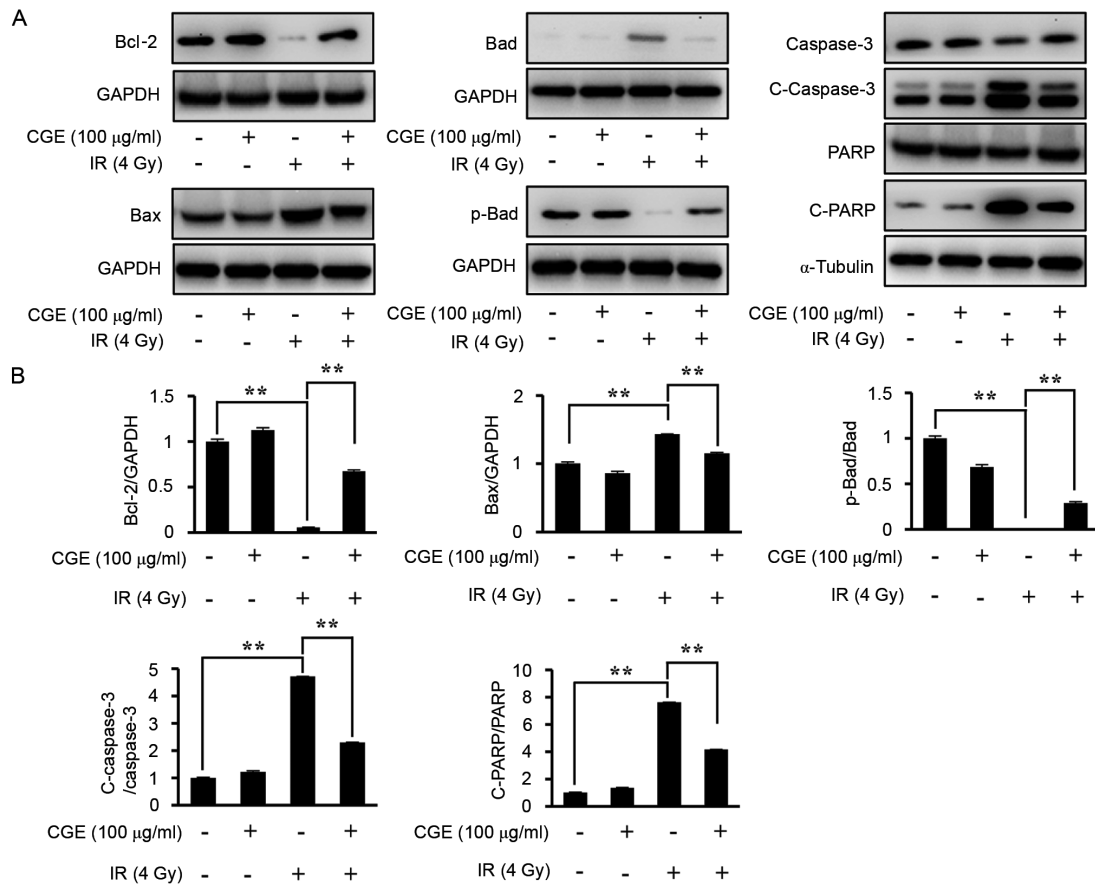
Figure 5. IR exposure-induced oxidative stress and CGE treatment resulted in altered apoptosis signaling in NIH-3T3 cells. (A) Lysates of IR-exposed cells in the presence or absence of CGE were immunoblotted with anti-Bcl-2, anti-Bax, anti-Bad, anti-p-Bad, anti-caspase-3, anti-C-caspase-3, anti-PARP, anti-C-PARP, or anti-GAPDH antibodies. (B) The western blots were analyzed quantitatively. Band intensities were normalized to those of the normal form of each protein, GAPDH, or α-tubulin. **P≤0.01 vs. IR only. IR, ionizing radiation; CGE, centipedegrass extract; Bcl-2, B-cell lymphoma-2; Bax, Bcl-2 like protein 4; p-, phosphorylated; Bad, Bcl-2-associated death promoter; PARP, poly(ADP-ribose) polymerase; GAPDH, glyceraldehyde 3-phosphate dehydrogenase; Con, vehicle control (0.1% DMSO); SD, standard deviation.
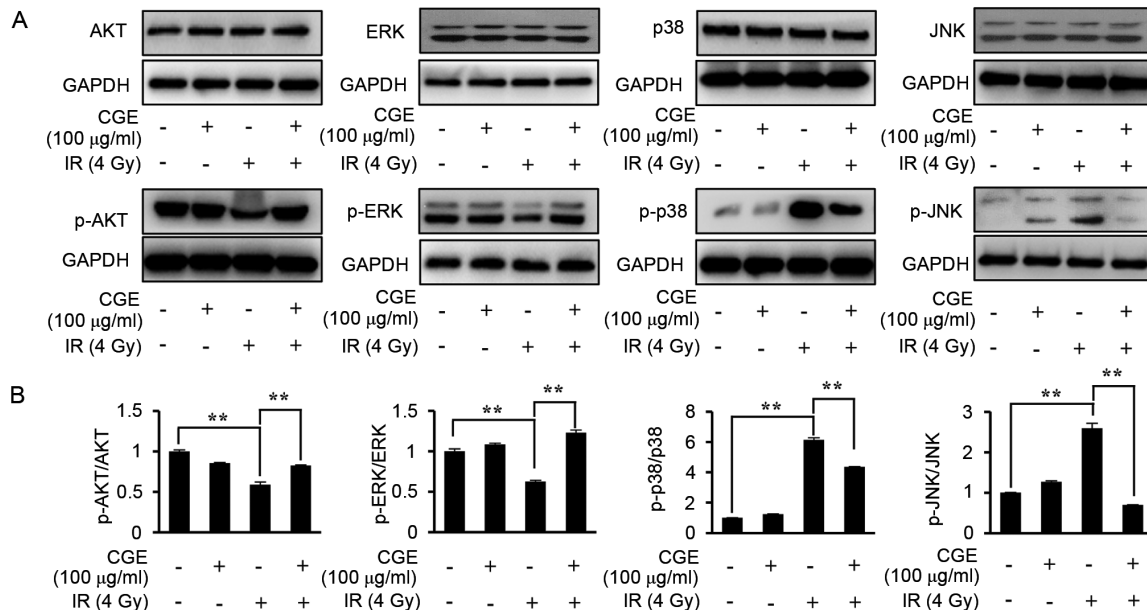

Figure 6. CGE inhibits apoptosis in IR-exposed NIH-3T3 cells by regulating the ERK-, p38-, JNK-MAPKs signaling. (A) Lysates of IR-exposed cells in the presence or absence of CGE were immunoblotted with anti-AKT, anti-p-AKT, anti-ERK, anti-p-ERK, anti-p38, anti-p-p38, anti-JNK, anti-p-JNK, or anti-GAPDH antibodies. (B) Western blots were analyzed quantitatively. The band intensities were normalized to those of the normal form of each protein or GAPDH. **P≤0.01 vs. IR only. CGE, centipedegrass extract; IR, ionizing radiation; p-, phosphorylated; ERK, extracellular-signal-regulated kinase; JNK, c-Jun N-terminal Kinase; MAPK, mitogen-activated protein kinase; AKT, protein kinase B; GAPDH, glyceraldehyde 3-phosphate dehydrogenase; Con, vehicle control (0.1% DMSO); SD, standard deviation.

and is essential for homeostasis in normal physiological levels; however, they function as toxic elements at aberrant levels and are associated with abnormal cell proliferation (26-28). IR strongly induces intracellular accumulation of ROS and RNS (29). Humans are exposed to natural sources of radiation such as those in water, soil, and vegetation, as well as those from human-made sources such as X-rays and medical devices (30). Notably, IR is used for RT, generally, as part of cancer treatment to control or kill malignant cells. However, some people undergoing RT experience dryness, itching, blistering, or peeling. This reversible effect depends on which part of the body has been exposed to radiation (31). One of the most common reversible effects is a skin condition called radiation dermatitis (32), in which, the ionizing radiation interacts directly or indirectly with the target macromolecules or water in cells leading to the occurrence of oxidizing events that alter cell molecular composition (29,33). In addition, oxidative damage can get extended from the target to neighboring non-target bystander cells through a redox-regulated intercellular proximity mechanism (34). Ultimately, the RT fails, resulting in unexpected damages to the cancer as well as normal cells due to IR-induced oxidative stress.

In a previously published study, maysin derived from corn silk was reported to increase cell viability under conditions of oxidative stress via upregulation of a neuronal antioxidative action (17). Conversely, it was reported that maysin (C-glycosyl flavone) isolated from the silks of *Zea mays* L. has a higher antioxidative activity than other compounds (rutin, quercetin, luteolin), thus, it has potential as a powerful antioxidant compound. In this study, the ability of CGE to rescue fibroblast cells from oxidative stress-induced apoptosis was demonstrated and the underlying effects were examined. In general, apoptosis has been recognized as an indication of cell death induced by oxidative stress followed by cell senescence (35). One of the most pivotal molecular pathways that are damaged by oxidative stress is that involving damage to the DNA (36). Previous studies have reported that DNA damage mediated by reactive oxygen intermediates causes enzymatic inactivation through cleavage of PARP, which is an important step in apoptosis (37). The function of cleaved PARP is to prevent repair of DNA strand breaks during apoptotic cell death, which is now widely known as the key marker of type 1 programmed cell death (38). PARP is cleaved by caspase-3 into two fragments of 89 and 24 kDa during apoptotic cell death in various cell lines (39). In this study, we demonstrated that CGE plays a role in cytoprotective effect on H_2O_2-induced cell death in mouse-derived fibroblasts. Pretreatment of NIH-3T3 cells with CGE (up to 100 μg/ml) before H_2O_2 treatment significantly attenuated cell death induced by oxidative stress, as observed by cell density and viability. CGE significantly inhibited PARP cleavage and prevented sustenance of DNA damage. Additionally, it was confirmed that CGE could significantly reduce the number of Annexin V- and PI-positive cells, indicating that pretreatment with CGE could significantly alleviate apoptosis induced by oxidative stress. Taken together, the results of this study suggest that due to its antioxidant activity, CGE has a cellular protective effect against oxidative stress-induced apoptosis in NIH-3T3 cells and may potentially act as a protective agent against IR-induced cell damage.

Furthermore, we have demonstrated that CGE pretreatment rescues NIH-3T3 cells subjected to IR exposure. Exposure to IR induced cell death and increased intracellular ROS levels; however, CGE pretreatment counteracted the cellular damages. In published reports, IR has been shown to activate three MAPKs (ERK1/2, p38, JNK MAPK pathway) in a cell type-dependent manner (25,40), and it has been shown that the phosphorylated JNK translocates to the nucleus, phosphorylates c-Jun (41,42). Phosphorylation of c-Jun leads to the formation of AP-1, JNK-AP-1 pathway is involved in the increased expression of pro-apoptotic genes (43). Our results have shown that pretreatment with CGE decreases the activation of JNK and p38 MAPKs followed by the apoptosis pathway. Taken together, these results indicated that CGE has protective effects against IR-induced apoptotic cell death and the mechanism underlying this effect is ROS scavenging and JNK-, ERK1/2-, p38-MAPK pathway modulation.

Several trials are being conducted to develop a radioprotector via the inhibition of p38 and JNK pathways in normal tissues, and some derivates from natural plants have shown protective effects against IR-induced ROS stress (44,45). In the previous study, it was reported that maysin (the major constituent of centipedegrass) not only plays a role as a ROS scavenger but also is able to increase the amount of antioxidant enzymes in a mammalian cell. Notably, in this study, CGE also exhibited protective effects against overwhelming ROS deposition induced by H_2O_2, and reduced the extent of apoptotic cell death induced by IR via downregulation of MAPK signaling (ERK, p38, JNK) in fibroblasts.

Therefore, CGE could be considered as an efficient radioprotector or a radiation palliative remedy, which could help reduce tissue damage induced by exposure to radiation in patients or sufferers unintentionally exposed to radiation or undergoing RT. However, to demonstrate the protective effect of CGE on skin tissue, experiments conducted with a single cell line derived from mice may be a limitation. To address this, human-derived skin cell experiments need to be performed. Additionally, in this study, the effects of individual constituents of CGE are still not be explored and should be explored in further studies. Furthermore, for the clinical application of any compound as a candidate for radiation protection, it is essential to avoid unacceptable clinical risks; therefore, absolute certainty about its safety for normal tissues is required. In laboratory studies, several compounds have been tested as radioprotectants; however, most did not reach the clinical stage due to the toxicity and side effects in animal models. Similarly, in this study, CGE was found to be non-toxic under normal conditions in fibroblasts; however, *in vivo* studies using animals with tumors are needed to investigate whether CGE has preferential radioprotective action in normal tissues over tumor tissues.

In conclusion, CGE contains C-glycosyl flavones and phenolic components, which protected mouse-derived fibroblasts from IR-induced apoptotic cell death by blocking ROS production and inhibiting ERK-, p38-, JNK-MAPKs signaling. Although large-scale animal studies and clinically relevant tests are needed to confirm the effectiveness of CGE, potential applications of CGE as a useful radioprotectant may be proposed.

Availability of data and materials

The datasets used and/or analyzed during the current study are available from the corresponding author on reasonable request.

Authors' contributions

SHK and DHB designed and performed the experiments. SSL and HWB interpreted the experimental results and drafted the manuscript. BYC and BSK performed the statistical analysis and revised the manuscript critically for important intellectual content. SHK and DHB confirmed the authenticity of all the raw data. All authors read and approved the final manuscript.

Ethics approval and consent to participate

Not applicable.

Patient consent for publication

Not applicable.

Competing interests

The authors declare that they have no competing interests.

References

1. Hirata M, Nagakura Y, Yuki N, Adachi K, Fujii R, Koyakumaru T, Ogura S, Moritake H, Watanabe C and Fukuyama K: Development and establishment of centipede grass (*Eremochloa ophiuroides*) in south-western Japan. Trop Grassl 41: 100-112, 2007.
2. Park HJ, Chung BY, Lee MK, Song Y, Lee SS, Chu GM, Kang SN, Song YM, Kim GS and Cho JH: Centipede grass exerts anti-adipogenic activity through inhibition of C/EBPβ, C/EBPα, and PPARγ expression and the AKT signaling pathway in 3T3-L1 adipocytes. BMC Complement Altern Med 12: 230, 2012.
3. Lee EM, Bai HW, Lee SS, Hong SH, Cho JY, Lee IC and Chung BY: Stress-induced increase in the amounts of maysin and maysin derivatives in world premium natural compounds from centipedegrass. Radiat Phys Chem 81: 1055-1058, 2012.
4. Lee EM, Lee SS, Bai H-W, Cho J-Y, Kim TH and Chung BY: Effect of gamma irradiation on the pigments and the biological activities of methanolic extracts from leaves of centipedegrass (*Eremochloa ophiuroides* Munro). Radiat Phys Chem 91: 108-113, 2013.
5. Liu J, Wang C, Wang Z, Zhang C, Lu S and Liu J: The antioxidant and free-radical scavenging activities of extract and fractions from corn silk (*Zea mays* L.) and related flavone glycosides. Food Chem 126: 261-269, 2011.
6. Choi DJ, Kim SL, Choi JW and Park YI: Neuroprotective effects of corn silk maysin via inhibition of H_2O_2-induced apoptotic cell death in SK-N-MC cells. Life Sci 109: 57-64, 2014.
7. Baskar R, Lee KA, Yeo R and Yeoh KW: Cancer and radiation therapy: Current advances and future directions. Int J Med Sci 9: 193-199, 2012.
8. Johung K, Saif MW and Chang BW: Treatment of locally advanced pancreatic cancer: the role of radiation therapy. Int J Radiat Oncol Biol Phys 82: 508-518, 2012.
9. Riley PA: Free radicals in biology: Oxidative stress and the effects of ionizing radiation. Int J Radiat Biol 65: 27-33, 1994.
10. Uttara B, Singh AV, Zamboni P and Mahajan RT: Oxidative stress and neurodegenerative diseases: A review of upstream and downstream antioxidant therapeutic options. Curr Neuropharmacol 7: 65-74, 2009.
11. Chan RJ, Webster J, Chung B, Marquart L, Ahmed M and Garantziotis S: Prevention and treatment of acute radiation-induced skin reactions: A systematic review and meta-analysis of randomized controlled trials. BMC Cancer 14: 53, 2014.
12. Bolderston A, Cashell A, McQuestion M, Cardoso M, Summers C and Harris R: A canadian survey of the management of radiation-induced skin reactions. J Med Imaging Radiat Sci 49: 164-172, 2018.
13. Wei J, Meng L, Hou X, Qu C, Wang B, Xin Y and Jiang X: Radiation-induced skin reactions: Mechanism and treatment. Cancer Manag Res 11: 167-177, 2018.
14. Chen J, Zhu Y, Zhang W, Peng X, Zhou J, Li F, Han B, Liu X, Ou Y and Yu X: Delphinidin induced protective autophagy via mTOR pathway suppression and AMPK pathway activation in HER-2 positive breast cancer cells. BMC Cancer 18: 342, 2018.
15. Zhang S and Duan E: Fighting against Skin Aging: The Way from Bench to Bedside. Cell Transplant 27: 729-738, 2018.
16. Panich U, Sittithumcharee G, Rathviboon N and Jirawatnotai S: Ultraviolet radiation-induced skin aging: The role of DNA damage and oxidative stress in epidermal stem cell damage mediated skin aging. Stem Cells Int 2016: 7370642-7370642, 2016.
17. Kim JH, Jenrow KA and Brown SL: Mechanisms of radiation-induced normal tissue toxicity and implications for future clinical trials. Radiat Oncol J 32: 103-115, 2014.
18. Smith TA, Kirkpatrick DR, Smith S, Smith TK, Pearson T, Kailasam A, Herrmann KZ, Schubert J and Agrawal DK: Radioprotective agents to prevent cellular damage due to ionizing radiation. J Transl Med 15: 232-232, 2017.
19. Painuli S and Kumar N: Prospects in the development of natural radioprotective therapeutics with anti-cancer properties from the plants of Uttarakhand region of India. J Ayurveda Integr Med 7: 62-68, 2016.
20. Mun GI, Kim S, Choi E, Kim CS and Lee YS: Pharmacology of natural radioprotectors. Arch Pharm Res 41: 1033-1050, 2018.
21. Badaboina S, Bai HW, Park CH, Jang DM, Choi BY and Chung BY: Molecular mechanism of apoptosis induction in skin cancer cells by the centipedegrass extract. BMC Complement Altern Med 13: 350, 2013.
22. Bindokas VP, Jordán J, Lee CC and Miller RJ: Superoxide production in rat hippocampal neurons: Selective imaging with hydroethidine. J Neurosci 16: 1324-1336, 1996.
23. Green DR and Kroemer G: The pathophysiology of mitochondrial cell death. Science 305: 626-629, 2004.
24. Hata AN, Engelman JA and Faber AC: The BCL2 family: Key mediators of the apoptotic response to targeted anticancer therapeutics. Cancer Discov 5: 475-487, 2015.
25. Dent P, Yacoub A, Fisher PB, Hagan MP and Grant S: MAPK pathways in radiation responses. Oncogene 22: 5885-5896, 2003.
26. Di Meo S, Reed TT, Venditti P and Victor VM: Role of ROS and RNS sources in physiological and pathological conditions. Oxid Med Cell Longev 2016: 1245049-1245049, 2016.
27. Schieber M and Chandel NS: ROS function in redox signaling and oxidative stress. Curr Biol 24: R453-R462, 2014.
28. Lee AY, Choi JM, Lee MH, Lee J, Lee S and Cho EJ: Protective effects of perilla oil and alpha linolenic acid on SH-SY5Y neuronal cell death induced by hydrogen peroxide. Nutr Res Pract 12: 93-100, 2018.
29. Azzam EI, Jay-Gerin JP and Pain D: Ionizing radiation-induced metabolic oxidative stress and prolonged cell injury. Cancer Lett 327: 48-60, 2012.
30. Canadian Nuclear Safety Commission (CNSC): Types and Sources of Radiation. Ottawa, ON, 2014.
31. Bray FN, Simmons BJ, Wolfson AH and Nouri K: Acute and chronic cutaneous reactions to ionizing radiation therapy. Dermatol Ther (Heidelb) 6: 185-206, 2016.
32. Leventhal J and Young MR: Radiation dermatitis: Recognition, prevention, and management. Oncology (Williston Park) 31: 885-887, 894-899, 2017.
33. Reisz JA, Bansal N, Qian J, Zhao W and Furdui CM: Effects of ionizing radiation on biological molecules - mechanisms of damage and emerging methods of detection. Antioxid Redox Signal 21: 260-292, 2014.

34. Mladenov E, Li F, Zhang L, Klammer H and Iliakis G: Intercellular communication of DNA damage and oxidative status underpin bystander effects. Int J Radiat Biol 94: 719-726, 2018.
35. Redza-Dutordoir M and Averill-Bates DA: Activation of apoptosis signalling pathways by reactive oxygen species. Biochim Biophys Acta 1863: 2977-2992, 2016.
36. Whitaker AM, Schaich MA, Smith MR, Flynn TS and Freudenthal BD: Base excision repair of oxidative DNA damage: From mechanism to disease. Front Biosci 22: 1493-1522, 2017.
37. Rodríguez-Vargas JM, Ruiz-Magaña MJ, Ruiz-Ruiz C, Majuelos-Melguizo J, Peralta-Leal A, Rodríguez MI, Muñoz-Gámez JA, de Almodóvar MR, Siles E, Rivas AL, *et al*: ROS-induced DNA damage and PARP-1 are required for optimal induction of starvation-induced autophagy. Cell Res 22: 1181-1198, 2012.
38. Ko HL and Ren EC: Functional Aspects of PARP1 in DNA Repair and Transcription. Biomolecules 2: 524-548, 2012.
39. Soldani C, Lazzè MC, Bottone MG, Tognon G, Biggiogera M, Pellicciari CE and Scovassi AI: Poly(ADP-ribose) polymerase cleavage during apoptosis: When and where? Exp Cell Res 269: 193-201, 2001.
40. Valerie K, Yacoub A, Hagan MP, Curiel DT, Fisher PB, Grant S and Dent P: Radiation-induced cell signaling: Inside-out and outside-in. Mol Cancer Ther 6: 789-801, 2007.
41. Davis RJ: Signal transduction by the JNK group of MAP kinases. In: Inflammatory Processes. Springer, pp13-21, 2000.
42. Chang L and Karin M: Mammalian MAP kinase signalling cascades. Nature 410: 37-40, 2001.
43. Fan M and Chambers TC: Role of mitogen-activated protein kinases in the response of tumor cells to chemotherapy. Drug Resist Updat 4: 253-267, 2001.
44. Santabárbara-Ruiz P, López-Santillán M, Martínez-Rodríguez I, Binagui-Casas A, Pérez L, Milán M, Corominas M and Serras F: ROS-induced JNK and p38 signaling is required for unpaired cytokine activation during Drosophila regeneration. PLoS Genet 11: e1005595-e1005595, 2015.
45. Choi EK, Yeo JS, Park CY, Na H, Lim J, Lee JE, Hong SW, Park SS, Lim DG and Kwak KH: Inhibition of reactive oxygen species downregulates the MAPK pathway in rat spinal cord after limb ischemia reperfusion injury. Int J Surg 22: 74-78, 2015.